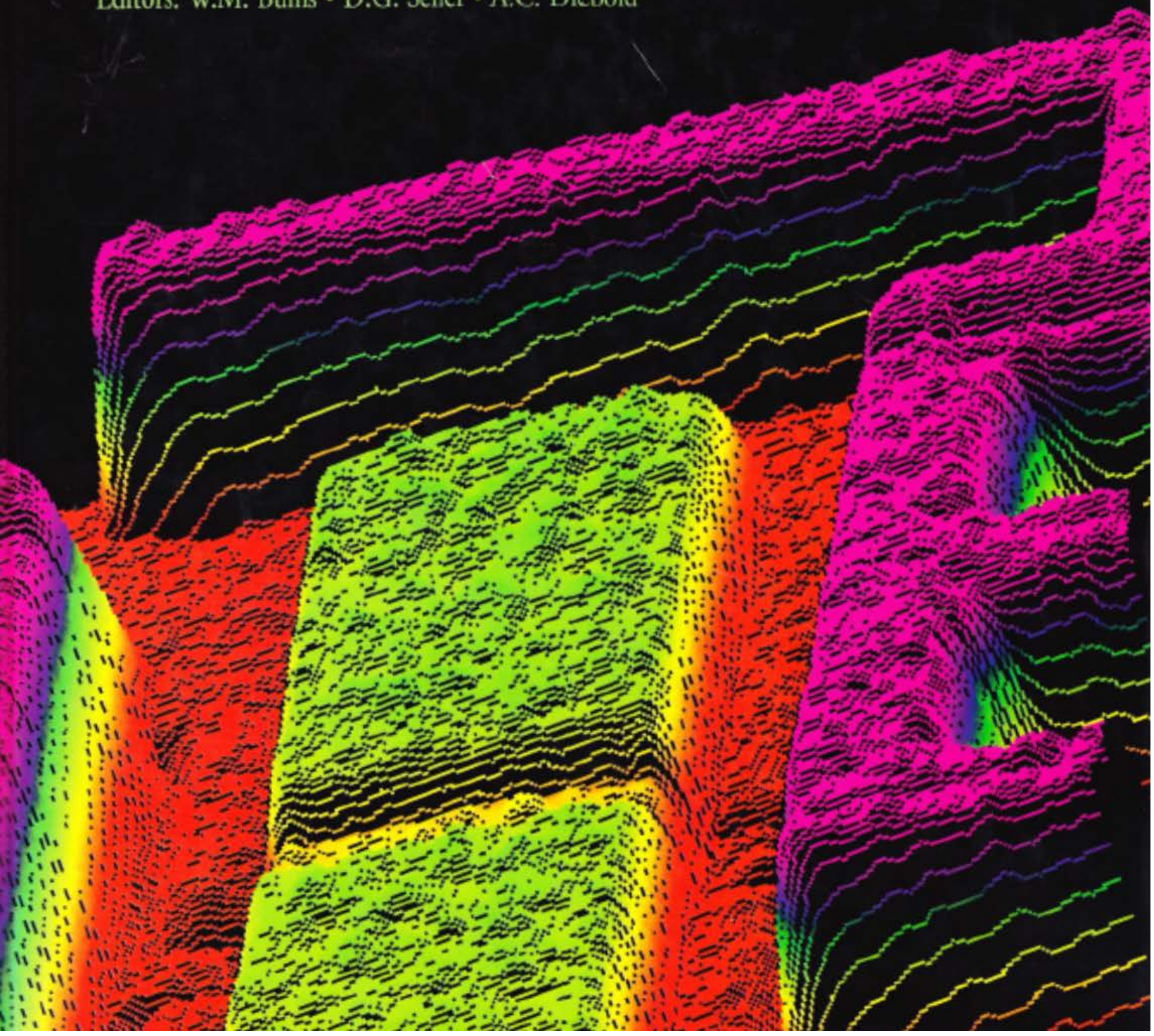


# Semiconductor Characterization

**Present Status and Future Needs**

Editors: W.M. Bullis • D.G. Seiler • A.C. Diebold



Proceedings of a Workshop at NIST, Jan. 30 - Feb 2, 1995,  
published by AIP 1996

**Semiconductor  
Characterization**  
**Present Status and Future Needs**

**EDITORS**

**W. M. Bullis**

*Materials & Metrology, Sunnyvale, CA 94087*

**D. G. Seiler**

*NIST, Gaithersburg, MD 20899*

**A. C. Diebold**

*SEMATECH, Austin, TX 78741*



# Energy Dispersive X-Ray Reflectivity Characterization of Semiconductor Heterostructures and Interfaces

E. Chason<sup>a)</sup>, T.M. Mayer<sup>a)</sup>, Z. Matutinovic Krstelj<sup>b)</sup> and J. C. Sturm<sup>b)</sup>

a) Sandia National Laboratories, Albuquerque, NM 87185-0350

b) Dept. of Electrical Engineering, Princeton U., Princeton, N.J. 08544

Energy dispersive X-ray reflectivity is a versatile tool for analyzing thin film structures. Layer thickness, interface roughness and composition can be determined with a single non-destructive measurement. Use of energy dispersive detection enables spectra to be acquired in less than 500 s with a rotating anode X-ray generator, making the study of kinetics possible.

Multiple advanced device structures incorporate thin semiconductor heterolayers to obtain enhanced performance, e.g., heterojunction bipolar transistors (HBT's), enhanced mobility FET's and resonant tunneling diodes. These structures require precise control of the layer thickness and interface morphology for optimal performance. We have developed a technique using energy dispersive X-ray reflectivity (XRR) to characterize these structures with high depth sensitivity. The parameters that can be determined from this measurement are layer thickness, composition and surface/interface roughness. Layer thickness can be determined in the range of 3 - 200 nm with  $\pm 5\%$  resolution and surface and interface roughness can be determined in the range of 0.1 - 3 nm with  $\pm 20\%$  resolution.

We have applied the XRR technique to characterize CVD-grown SiGe/Si hetero-structures [1], enabling us to correlate the layer thickness and interface roughness with the growth conditions. We have also performed real-time measurements during low-energy ion sputtering of semiconductors [2,3] and SiO<sub>2</sub> [4] to determine the kinetics of surface evolution. These measurements confirmed the presence of a rapid roughening instability and enabled us to quantitatively determine the value of ion-enhanced transport parameters (diffusivity, viscosity) important for sputter-morphology evolution.

## PRINCIPLES OF X-RAY REFLECTIVITY

The origin of XRR is treated in a number of publications, both in an optical multilayer [5] and a

diffraction formalism [6], so only a brief treatment will be presented here. X-ray reflectivity is defined as the ratio of the reflected intensity to the incident intensity and is measured as a function of the scattering vector,

$$k = 4\pi/hc E \sin\theta \quad (1)$$

where  $E$  is the energy of the X-ray and  $2\theta$  is the scattering angle. In contrast with X-ray diffraction, X-ray reflectivity is performed at small values of  $k$  where the reflectivity can be interpreted using the Fresnel equations. The layer is treated as a continuous medium with an index of refraction,  $n$ , that depends on the electron density,  $\rho_{el}$  [7]. The index of refraction for X-rays in matter is less than 1 so that for sufficiently small incident angles total external reflection occurs.

Above the critical value for total external reflection ( $k_c$ ), the reflectivity from an ideal interface is given by the Fresnel reflectivity ( $R_F(k)$ ) with the asymptotic form  $(k/k_c)^{-4}$ . For an imperfect interface, the reflectivity is given approximately by [6]

$$R(k) = R_F(k) |F(d\rho_{el}/dz)|^2 \quad (2)$$

where  $F(d\rho_{el}/dz)$  is the Fourier transform of the electron density gradient in the direction normal to the surface of the film. It is important to note that this equation refers to the specular reflectivity, i.e., where the angle of incidence equals the angle of reflection. Under these conditions, the scattering vector is oriented normal to the surface so that the reflectivity is only sensitive to variations in the electron density normal to the film

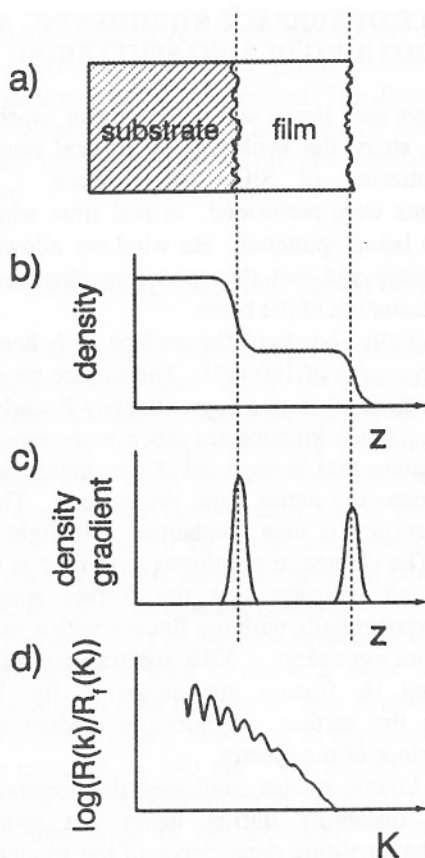


Figure 1. Relationship between thin film structure and X-ray reflectivity as expressed in eq. (2). a) Film structure consisting of homogeneous layer on substrate. b) Electron density normal to surface corresponding to structure in (a). c) Gradient in electron density showing peaks at interfaces (indicated by dotted lines). d) Reflectivity derived from Fourier transform of electron density gradient normalized by Fresnel reflectivity.

surface and does not probe the interface structure in the plane of the film.

The relationship expressed in eq. (2) between the thin film and the reflectivity is shown schematically in figure 1. The structure consists of a single uniform layer on a substrate (fig. 1a). The electron density in the direction normal to the film surface (fig. 1b) is constant where the film composition is uniform and changes at the interfaces between the substrate, the film and vacuum. The gradient of the electron density ( $d\rho_{e1}/dz$ ) has peaks at these interfaces as shown in fig. 1c. If the interface is smooth, then the peak in  $d\rho_{e1}/dz$  will be narrow, while if the interface is rough or diffuse, the peak will be broader.

The normalized reflectivity ( $R(k)/R_F(k)$ ) from this structure (fig. 1d) is given by the Fourier transform of the density gradient. The oscillations shown in the

reflectivity spectra come from interference between scattering from the surface and the buried interface. The period of the oscillations is inversely proportional to the layer thickness. The decay in the reflected intensity is determined by the roughness of the interfaces. For rough interfaces, the reflectivity decreases faster with increasing  $k$  than for sharp interfaces. The roughness is generally taken to have a Debye-Waller form ( $\exp(-k^2\sigma^2)$ ) where  $\sigma$  is the interface roughness.

## EXPERIMENTAL TECHNIQUE

The details of the experimental apparatus are shown in figure 2. The X-ray source is a rotating anode generator operated at 40 kV, 100 mA. In the energy dispersive technique used in this work, the broad range of X-ray energies produced by Bremsstrahlung radiation from a Mo anode impinge simultaneously on the sample at a fixed angle. A solid-state Ge detector is used to measure the reflectivity at each energy and the energy spectrum is converted to wavevector using eq. 1. In order to obtain the reflectivity, the measured spectra is normalized by the incident energy spectrum.

The X-ray beam is incident on the sample at a grazing incidence angle between 0.4 and 1.0 deg. The angular divergence of the ingoing and outgoing beam is typically on the order of 0.01 deg as defined by slits. The angular resolution is chosen to match the energy resolution of the Ge detector, approximately 1-2 % in the energy range of 8 - 35 KeV used. The total area of the sample illuminated by the X-ray beam is approximately  $0.5 \times 0.5 \text{ cm}^2$ ; the lateral coherence length of the X-rays is on the order of  $1 \mu\text{m}$ .

There are several advantages to energy dispersive detection over conventional angle scanning for in situ measurements. The fixed angle of incidence means that the sample does not have to be moved during the measurement. The fixed angle also means that the footprint of the beam on the sample is constant so no corrections need to be made for low  $k$  values. By using

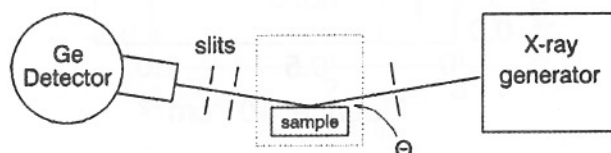


Figure 2. Schematic of apparatus for energy dispersive X-ray reflectivity measurements.

## KINETICS OF SURFACE ROUGHENING AND SMOOTHING DURING SPUTTERING

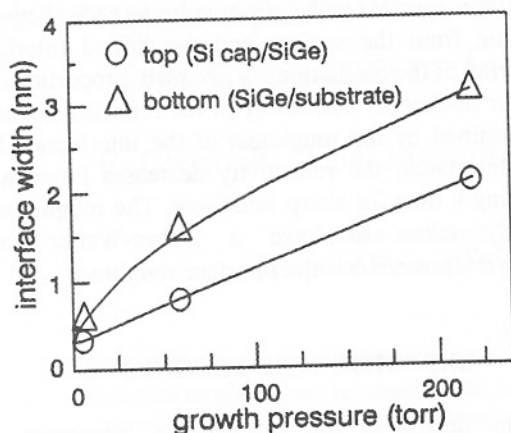


Figure 4. Dependence of roughness on growth pressure for top (Si cap/SiGe) and bottom (SiGe/Si substrate) interfaces. The spectra were fit to a two-layer model; the calculated intensity from the multilayer model is shown as the dashed line in the figures. The intensity of the oscillations in the spectra decreases for the samples grown at higher pressures.

Analysis of these spectra indicate that the decrease in the oscillation intensity corresponds to increased roughness at the interfaces. The roughness at the SiGe/substrate interface and the SiGe/Si cap interface is shown in figure 4 as a function of growth pressure. The increase in surface roughness with increasing growth pressure was determined to be caused by the presence of graded layers at the interfaces created by a transient in the switching time of the gases in the growth reactor. This discovery was used to determine growth conditions to produce more abrupt interfaces.

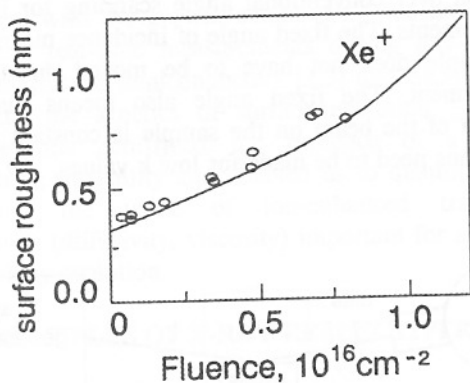


Figure 5. Kinetics of  $\text{SiO}_2$  surface roughening induced by low energy Xe sputtering. Line represents fit to model of sputter-induced roughening instability.

We have used the in situ measurement capabilities of XRR to study the evolution of surface roughness during sputtering of  $\text{SiO}_2$  [4] surfaces. These measurements were performed in real time while the surface was being sputtered. Be windows allowed the X-rays to enter and exit the sputtering chamber with minimal attenuation of the beam.

We initially bombard the surface with heavy Xe ions with an energy of 1000 eV. The surface roughness is shown in figure 5 to rise approximately linearly with ion fluence. These kinetics are much more rapid than the  $t^{1/2}$  behavior that is expected if the sputter beam is randomly removing atoms from the surface. The Xe-roughened surface is then bombarded with light (H or He) ions. The change in roughness with time is shown in fig. 6 and indicates that the surface roughness decreases exponentially with ion fluence with a rate that increases with ion energy. XRR spectra corresponding to increasing He fluence are shown in fig. 7; the decrease in the surface roughness is evident by the decreasing slope of the spectra.

These kinetic studies confirmed the presence of a roughening instability during heavy ion sputtering caused by the curvature dependence of the sputter yield that leads to much more rapid roughening than a simple stochastic removal process. The smoothing by light ions was due to ion-enhanced viscous flow of the oxide. Although in principle similar measurements could be obtained by sequences of AFM measurements, these would be very difficult to obtain. The real time capability of the XRR provided critical kinetic data for

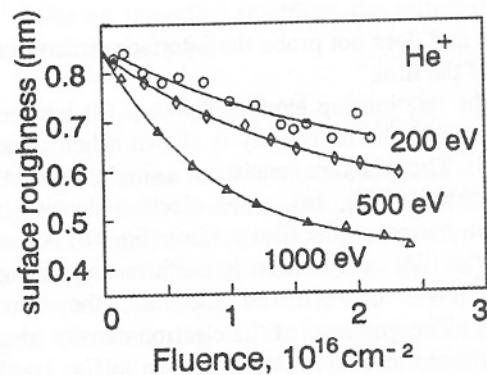


Figure 6. Decrease in surface roughness during He sputtering of  $\text{SiO}_2$ . Surfaces were initially roughened by Xe sputtering. Lines show fit to exponential decay due to ion-enhanced viscous flow.

the Bremsstrahlung radiation, spectra can be obtained from a laboratory-based X-ray generator in less than 500 s so that kinetics can be measured. The disadvantages to energy dispersive detection are reduced resolution and possible interference by X-ray fluorescence from the sample.

### XRR ANALYSIS AND SENSITIVITY

For analysis of the reflectivity spectra, an optical multilayer model that takes into account multiple scattering is used. Optimum values of parameters corresponding to layer density, thickness, surface roughness and buried interface roughness are obtained using a non-linear least-squares fitting routine. It is generally impractical to model a structure containing more than two layers unless some of the parameters can be determined by alternative means.

The sensitivity of the least squares fit to changes in the parameters is used to obtain a value for the error associated with each parameter. The layer thickness can be determined with a resolution of approximately  $\pm 5\%$  in the range of 3 - 200 nm. The surface and interface roughness can be determined in the range of 0.1 - 3 nm with a resolution of approximately  $\pm 20\%$  of the roughness. For smooth surfaces, this implies a roughness sensitivity of  $\pm 0.02$  nm. The determination of electron density is strongly coupled to the degree of roughness, but typical sensitivity is on the order of  $\pm 30\%$ .

### XRR CAPABILITIES AND COMPARISON WITH OTHER TECHNIQUES

It is useful to compare XRR with other thin film analytical techniques to determine its advantages and disadvantages. The greatest strength of XRR is the ability to measure thickness, density and roughness in a single measurement. Because the X-rays are highly penetrating, buried layer interfaces can be probed as well as surface roughness. The technique is non-destructive and requires no special sample preparation. The glancing incidence geometry does not interfere with deposition and other processing techniques. Ambient gas processing environments are not a problem since the technique does not require a vacuum like electron diffraction does. The measurement averages over a large area instead of a small fraction of the sample like cross-sectional transmission electron microscopy (XTEM) or scanning probe microscopies (AFM, STM). The depth sensitivity is very high compared to other probes like

Rutherford backscattering (RBS). The technique can be employed in situ and using energy dispersive detection, spectra can be obtained in less than 500 s making studies of kinetics possible. In comparison with ellipsometry, the optical properties of the layers depend only on the total electron density and can be more easily modeled.

The primary drawbacks to the technique are that parameters can not be obtained directly and the measured spectra need to be fit to an optical multilayer theory. This makes the uniqueness of the parameter set obtained difficult to determine, especially for more complicated structures. In comparison with imaging techniques such as XTEM and STM, XRR provides no information about the in-plane structure of the layers.

### CVD GROWTH OF SiGe HETEROSTRUCTURES

We have used XRR to characterize heterostructures of SiGe grown by CVD. Further details of the growth apparatus and experimental conditions can be found in ref 1. The structures consisted of a Si substrate, a SiGe layer and a Si cap. In figure 3, we show the reflectivity spectra from three samples grown at different pressures (the zeroes of the curves have been displaced for clarity).

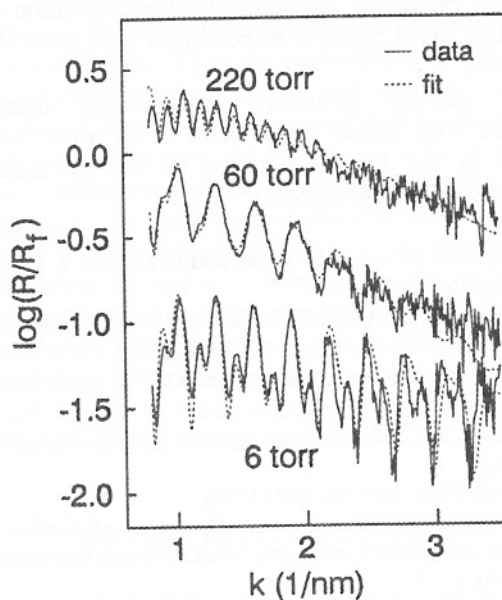


Figure 3. XRR spectra from CVD-grown heterostructures consisting of Si cap/SiGe/Si substrate. Dashed lines represent fit to optical multilayer model. Growth pressure indicated on figure.

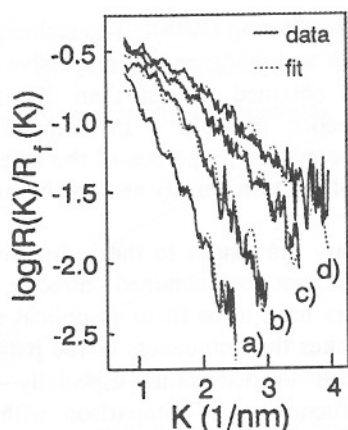


Figure 7. XRR spectra from  $\text{SiO}_2$  surfaces smoothed by low energy He sputtering. Increasing ion fluence from a) to d). Dashed lines represent fit to optical multilayer model.

development of models of surface roughening and smoothing.

In summary, XRR is a useful in situ probe of semiconductor thin films. It provides information about layer thickness, composition and interface roughness with sensitivity in the nanoscale regime that is becoming increasingly important technologically. Simple non-destructive sample preparation, relatively rapid data acquisition and compatibility with deposition geometries make it suitable for in situ kinetic studies of morphology evolution. For complete characterization of the structure, XRR needs to be combined with other in-plane probes.

The authors gratefully acknowledge useful discussions with Bruce Kellerman. This work was supported by the U.S. Department of Energy under contract DE-ACO4-94AL85000.

1. Z. Matutinovic-Krstelj, J.C. Sturm and E. Chason, *J. Elect. Mater.*, submitted.
2. E. Chason, T.M. Mayer, B.K. Kellerman, D.N. McIlroy and B.K. Kellerman, *Phys. Rev. Lett.* **72**, 3040 (1994).
3. E. Chason, T.M. Mayer, A. Payne and D. Wu, *Appl. Phys. Lett.* **60**, 2353 (1992).
4. T.M. Mayer, E. Chason and A.J. Howard, *J. Appl. Phys.* **76**, 1633 (1994).
5. L.G. Paratt, *Phys. Rev.* **95**, 359 (1954)
6. J. Als-Nielsen in *Structure and Dynamics of Surfaces*, edited by W. Schommers and P. von Blanckenhagen (Springer, Berlin, 1986), p. 181.
7. J.H. Underwood and T.W. Barbee, *Appl. Opt.* **20**, 3027 (1981).